Near-infrared lateral photovoltaic effect of epitaxial $LaTiO_{3+\delta}$ films under high pressure

Jianfeng Xi (息剑峰)[1,2], Kun Zhao (赵 昆)[2,*], Hao Ni (尼 浩)[2], Wenfeng Xiang (相文峰)[2], and Lizhi Xiao (肖立志)[1]

[1]*State Key Laboratory of Petroleum Resources and Prospecting, China University of Petroleum, Beijing 102249, China*
[2]*Beijing Key Laboratory of Optical Detection Technology for Oil and Gas, China University of Petroleum, Beijing 102249, China*
**Corresponding author: zhk@cup.edu.cn*

Received July 12, 2015; accepted November 19, 2015; posted online December 24, 2015

A lateral photovoltaic effect (LPE) is discovered in an $LaTiO_{3+\delta}$ film epitaxially grown on a (100) $SrTiO_3$ substrate. Under the illumination of a continuous 808 nm laser beam that is focused on the $LaTiO_{3+\delta}$ film through the $SrTiO_3$ substrate, the open-circuit photovoltage depends linearly on the illuminated position. The sensitivity of the LPE can be modified by the bias current. The $LaTiO_{3+\delta}$ film shows a stable photoelectric property under the high pressure, up to 9 MPa. These results indicate that the $LaTiO_{3+\delta}$ films can give rise to a potentially photoelectronic device for near-infrared position-sensitive detection in high-pressure environments.

OCIS codes: 310.6870, 230.5160, 040.5350.
doi: 10.3788/COL201614.013101.

Recent advances in the design of artificial transition-metal oxides[1] have vastly expanded the range of materials in which electronic interface phenomena can be systematically studied and controlled. At the interfaces between the two band insulators $LaAlO_3$ and $SrTiO_3$ (STO), several interesting physical phenomena have been reported, including a metal-insulator transition[2], electric-field tunable switching[3], magnetic correlations[4], and two-dimensional superconductivity[5,6]. Since bulk transition-metal oxides show a large variety of competing ground states and diverse physical properties due to their strong electron correlations, incorporating such complex oxide films provides additional opportunities for generating novel phenomena[7,8]. The Mott insulator $LaTiO_3$ embedded in the band insulator STO has been studied recently. The investigations of $LaTiO_3$/STO have been focused on their electro-optical properties[9–14]. Now, we focus on its application in the field of petroleum energy. Optical techniques are being used for a number of applications in the oil and gas markets, where very specific demands must be met to ensure the utmost in safety, productivity, and harsh environment durability. The development of a down-hole optical well-logging video system aimed at solving the key techniques of high-temperature resistance and high-pressure resistance, can have an important effect in detecting the structure of oil and gas wells. Within wells, the high-pressure environmental conditions are challenging. The well testing results of the conventional optical sensors under high pressure demonstrated that the probability of losing efficacy for the components has clearly increased.

The lateral photovoltaic effect (LPE) discovered by Schottky in 1930 has been widely used, as position-sensitive detectors in many fields require precision measurements[15]. In order to improve the sensitivity and linearity of position-sensitive detectors, many researchers have made efforts to study LPE in various kinds of materials systems, such as conventional p-n junctions, hydrogenated amorphous silicon-based structures, porous silicon, etc[16–21]. Almost all of the reported LPEs were applied in the visible or ultraviolet region, while works concerning large LPEs in the near-infrared region are rarely reported. In this Letter, we have grown epitaxial $LaTiO_{3+\delta}$ (LTO) films on STO substrates using pulsed laser deposition (PLD) technique, and present a near-infrared LPE by irradiating the structure of the LTO/STO. The open-circuit photovoltage of the LTO film depended linearly on the illuminated 808 nm laser beam position. The sensitivity of the LPE can be modified with the bias current. The LTO film shows a stable photoelectric property under the high pressure. The results demonstrate that the present film has a great potential application in near-infrared position-sensitive detectors in high-pressure environments.

The LTO film was grown on the STO substrate by PLD with *in-situ* monitoring by reflection high-energy electron diffraction. The PLD system used in this study was equipped with a KrF excimer laser (248 nm). The residual pressure of the chamber was less than 10^{-8} mbar. The STO (001) substrate was cleaned in methanol before its introduction into the vacuum chamber. During the deposition, oxygen gas was introduced to the chamber at a pressure of approximately 0.01 mbar. The substrate temperature was 1123 K. The laser pulse repetition rate was 2 Hz at a pulsed energy of 400 mJ and an energy density of 3.5 J/cm^2. The thickness of the LTO film was approximately 100 nm. X ray diffraction (XRD) was adopted to characterize and analyze the phase purity and crystal structure of the as-deposited LTO film.

The sample geometry is 5 mm × 5 mm, with a thickness of 0.5 mm. Before the experiments, the sample was cleaned carefully using a routine cleaning process that involved an ultrasonic cleaner in acetone and ethanol. For the photoresponse measurement, two Ag electrodes with the size of 1 mm × 4 mm separated by 3 mm were painted on the laser-irradiated surface of the LTO film, as shown in the inset of Fig. 1(a). As we can see from Fig. 1(a), the resistance of the LTO sample increased when the 808 nm laser irradiated the sample. This is because the LTO film we prepared is oxygen redundant. The resistance of the whole LTO film is about 600 Ω. The electrical property of the LTO film is metallic. So the carrier mobility in the LTO film decreased when the laser irradiated the sample. That induced the resistance of LTO film to become large when the laser irradiated the sample. The ohm contact between Ag and LTO is confirmed by the linear current-voltage (I-V) characteristics, as shown in Fig. 1(a). The continuum solid-state laser at wavelengths of 808 nm was used to irradiate the LTO film perpendicularly. Laser-induced I-V characteristics were measured by a sampling oscilloscope of 350 MHz terminated into 1 MΩ at an ambient temperature.

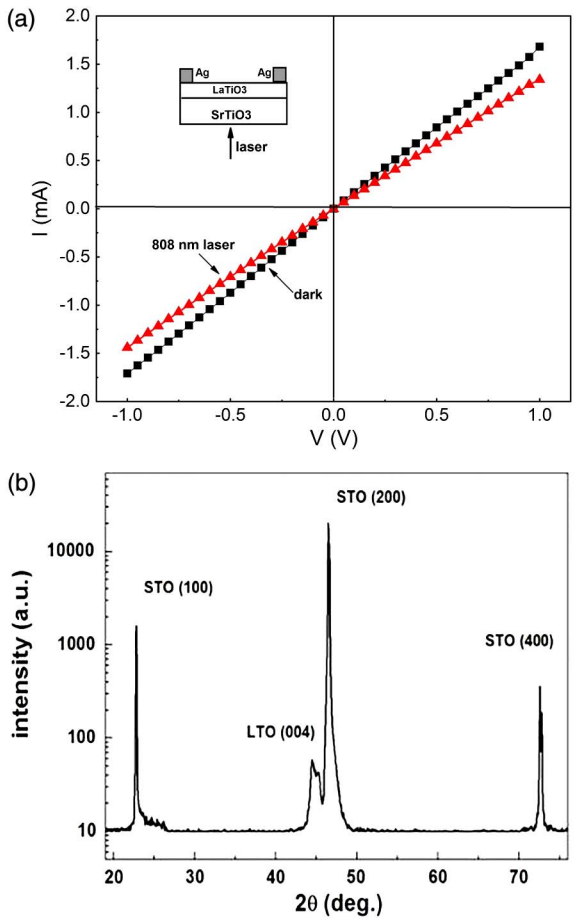

Fig. 1. (a) Typical I-V characteristics of the LTO/STO at room temperature. The insets show the schematic measurement setup. (b) XRD pattern of LTO/STO sample.

The microstructure of the LTO/STO sample was checked with an XRD $2\theta-\theta$ scan [Fig. 1(b)]. Except for the peaks of the (100) STO, the as-deposited sample exhibits the expected (001)-oriented perovskite structure with no diffraction peak from the impurity phase or randomly oriented grain. This implies that the LTO film is a single phase and [001] oriented.

Figure 2(a) shows the typical waveforms recorded by the oscilloscope when the 808 nm laser irradiated the LTO film through the STO substrate at different positions. The on-sample laser power is 120 mW. The electrodes on the sample were blocked in order to rule out the situation of the laser irradiating the electrodes. When the laser irradiated the sample, the lateral photovoltage (LPV) rises fast for about 3 s and then stabilizes. We define the position 0 mm as the center of the LTO sample, which is 1.5 mm away from each electrode. The moving axis of the laser spot is perpendicular to the electrodes. The LPVs at the positions of 1.5 and −1.5 mm were 5.9 and −5.8 mV, respectively. The LPV was dramatically changed when the laser irradiated different positions. Figure 2(b) shows the LPV as a function of the laser spot

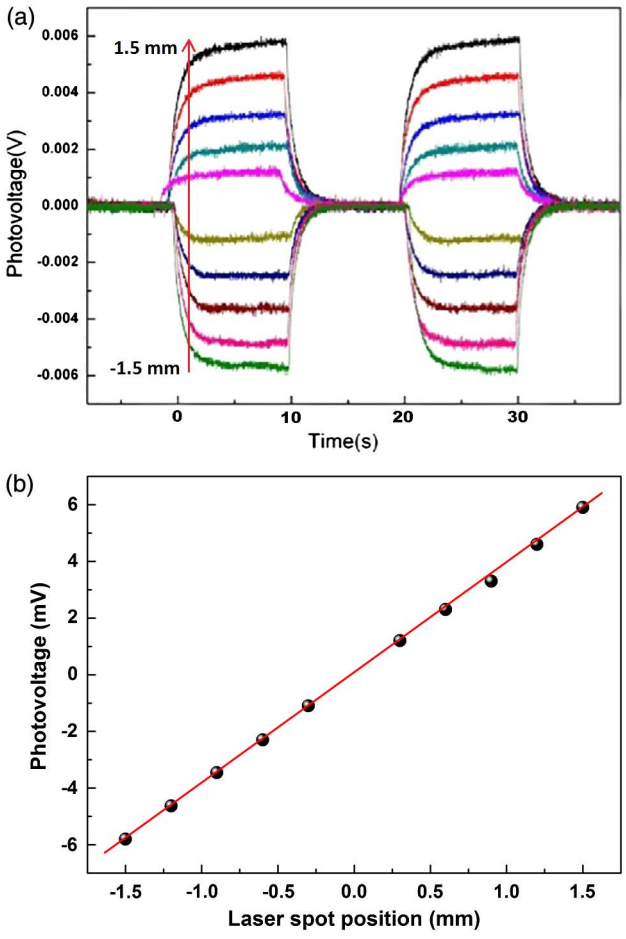

Fig. 2. (a) Typical waveforms recorded by oscilloscope with 1 MΩ input impedance without any bias when laser spot irradiated the region from position 1.5 mm to position −1.5 mm. (b) Steady waveforms' peak voltages depended linearly on the spot positions.

position. It is clear that the photovoltage shows a good linear relationship with the illuminated position. The position sensitivity of the LPV in the sample is about 3.9 mV/mm. The band gap of the LTO is ~1.2 eV[22], so electrons were excited from the valance band to the conduction band by absorbing the photon energy when the 808 nm laser irradiated the sample. The light-induced non-equilibrium electrons in the LTO will generate a lateral gradient between the illuminated and non-illuminated zones, resulting in excess electrons diffusing laterally along the film away from the illuminated spot toward two sides (at anode and cathode). When the lateral distance of the laser spot from each contact is different, the electron density impacting the built-in electric field is different. Thus, an LPV is generated to be proportional to the difference of the electron density between two lateral electrodes and strongly dependent on the laser spot position.

To investigate the influence of the laser power in the LPV measurements, the photovoltages of the LTO sample at the position of 1.5 mm were measured when the 808 nm laser irradiated the sample at different powers. The voltage value changed from 0.5 to 6.7 mV under the radiant laser power, which ranged from 7.8 to 131 mW, as shown in Fig. 3(a). As we can see from Fig. 3(b), the voltage value shows a good linear relationship with the radiant laser power. That means that the position sensitivity of the LPV is stable in the LTO sample.

To further improve the sensitivity of the LPV in the LTO sample, we measured the photovoltages by gradually increasing the bias current from 0 to 350 μA under 808 nm laser illumination at the position of 1.5 mm. The power of the laser is 120 mW. Figure 4(a) shows the baseline value of the oscilloscope at the laser-off state and the photo-induced voltage, both of which increased as the bias current increased from 0 to 350 μA. As we can see from Fig. 4(b), the photovoltage of the LTO sample increased steadily from 5.9 to 46.2 mV as the bias current increases from 0 to 350 μA. Therefore, we may conclude that the bias current plays a significant role in the sensitivity of the LPV in the LTO sample.

We measured the LPE in a high-pressure environment to investigate whether or not the LTO film is stable when the LPE occurred in the sample. The photovoltages of the LTO sample at the position of 1.5 mm were measured when the 808 nm laser irradiated the sample under

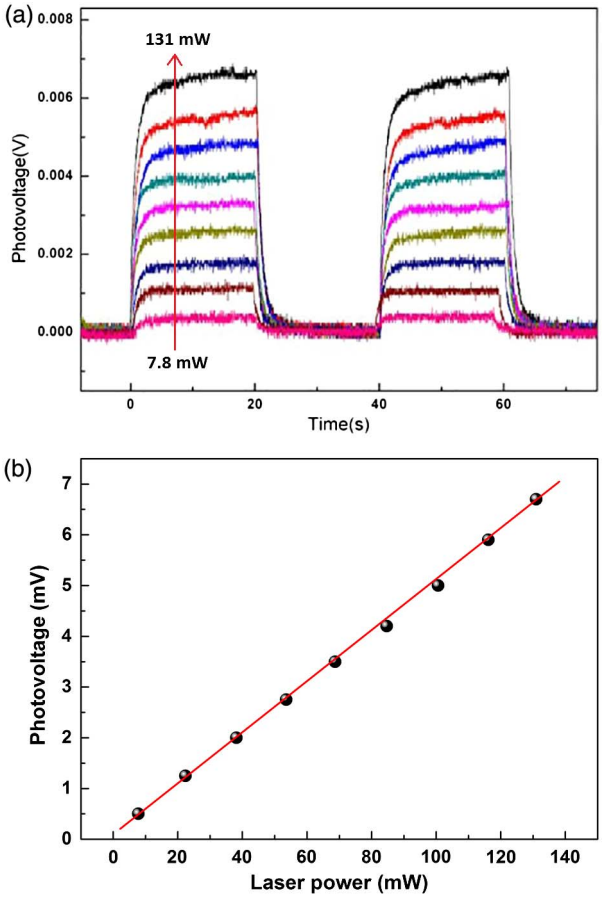

Fig. 3. (a) Typical waveforms with different on-sample laser power from 7.8 to 131 mW at position of 1.5 mm. (b) LPV dependence on the on-sample laser power.

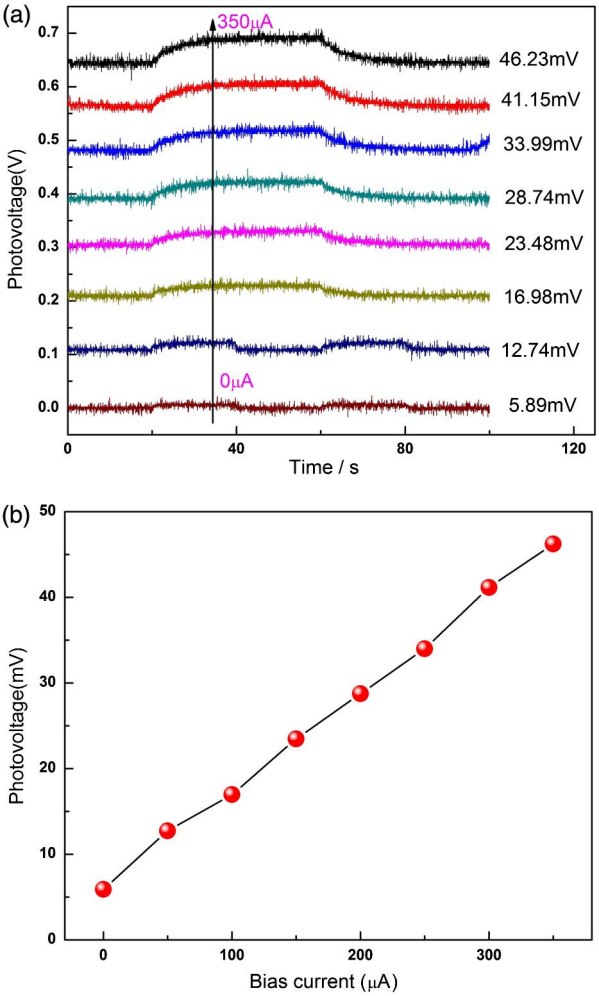

Fig. 4. (a) Typical waveforms with bias currents applied from 0 to 350 μA at the position of 1.5 mm. (b) Laser-induced photovoltage dependence on the bias current.

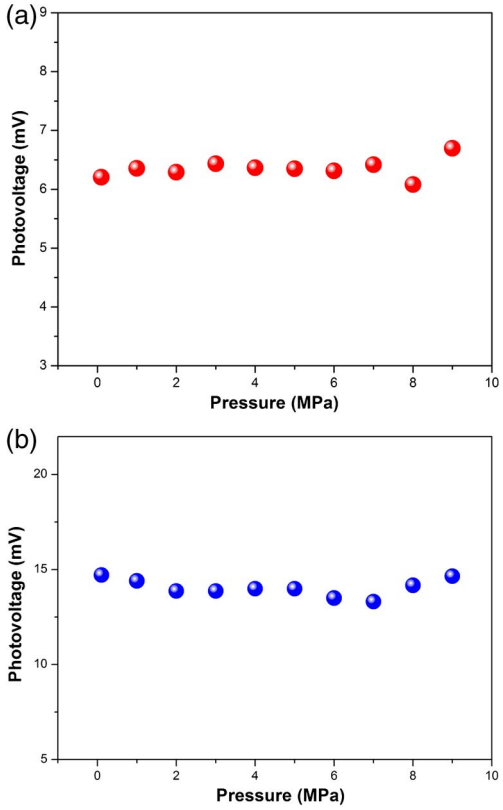

Fig. 5. (a) Laser-induced photovoltages under different pressures with a 1 mA bias current. (b) Laser-induced photovoltages under different pressures with a 3 mA bias current.

atmospheric pressure ranging from 0.1 to 9 MPa. The laser power decayed a lot when the laser traveled through the quartz glass window of the autoclave. The efficient signals of the LPVs cannot be obtained because the laser power is too low. From our previous experiments, the bias current can enlarge the signal of the LPV. So we measured the photovoltages at different pressures with 1 and 3 mA bias currents to check the stability of the LTO film under the LPE. It can been seen in Fig. 5(a) that the maximum and minimum of the photovoltages that measured with 1 mA bias current under the pressure, which were increased from 0.1 to 9 MPa, are 6.7 and 6.2 mV, respectively. The change rate of the photovoltage is below 8%. Figure 5(b) shows the photovoltages are in the region from 13.5 to 15 mV with the 3 mA bias current when the pressure increased from 0.1 to 9 MPa. The change rate of the photovoltage is below 10%. From these results, we conclude that the laser-induced voltage characteristic of the LTO film is stable under high pressure.

At present, tools that can effectively manage the environmental and financial risks associated with the operation of oil wells' production facilities have become of paramount importance, and non-destructive detecting techniques for oil wells are required. Among these techniques, optical sensors are an effective permanent and real-time solution for logging. The photodetectors based on LTO films show the ability to operate in high-pressure environments. As shown in Fig. 2, the position sensitivity of the LPV of the LTO film can be as high as 3.9 mV/mm. This is a large LPV in the near-infrared region because it is hard to absorb the light in this region. In addition, we made a detailed study of the LPV response to different bias currents and laser powers. The results show that the position sensitivity of the LPV has a dual dependence on both the laser power and bias current. This will help to improve the LPV position sensitivity of the LTO films that are made into photodetectors. The LTO film shows stable photovoltaic properties in a high-pressure environment, suggesting the potential application of LTO film photodetectors in harsh environments. To meet the challenges of applying the LTO in near-infrared position-sensitive detection, further research, such as of the slow response time, is currently in progress.

In conclusion, we report the LPE in an LTO film on an STO substrate when an 808 nm laser irradiates the sample. The photoelectric properties of the LPE in the LTO film are stable under high pressures. The sensitivity of the LPE can be tuned by the bias current. The experimental results show that the LTO film possesses potential applications for near-infrared position-sensitive photodetectors under normal and high pressure.

This work was supported by the National 973 Program of China (No. 2014CB744302) and the Specially Founded Program on National Key Scientific Instruments and Equipment Development (No. 2012YQ140005).

References

1. A. Ohtomo, D. A. Muller, J. L. Grazul, and H. Y. Hwang, Nature **419**, 378 (2002).
2. H. N. Lee, H. M. Christen, M. F. Chisholm, C. M. Rouleau, and D. H. Lowndes, Nature **433**, 395 (2005).
3. S. Thiel, G. Hammerl, A. Schmehl, C. W. Schneider, and J. Mannhart, Science **313**, 1942 (2006).
4. A. Brinkman, M. Huijben, M. Van Zalk, J. Huijben, U. Zeitler, and J. C. Maan, Nat. Mater. **6**, 493 (2007).
5. N. Reyren, S. Thiel, A. D. Caviglia, L. Fitting Kourkoutis, G. Hammerl, C. Richter, C. W. Schneider, T. Kopp, A.-S. Rüetschi, D. Jaccard, M. Gabay, D. A. Muller, J.-M. Triscone, and J. Mannhart, Science **317**, 1196 (2007).
6. A. D. Caviglia, S. Gariglio, N. Reyren, D. Jaccard, T. Schneider, M. Gabay, S. Thiel, G. Hammerl, J. Mannhart, and J.-M. Triscone, Nature **456**, 624 (2008).
7. S. Okamoto and A. J. Millis, Nature **428**, 630 (2004).
8. F. Zhang, Q. Zhang, B. Wang, D. Hu, H. Yu, H. Zhang, Z. Wang, and X. Xu, Chin. Opt. Lett. **12**, 121902 (2014).
9. S. Okamoto, A. J. Millis, and N. A. Spaldin, Phys. Rev. Lett. **97**, 056802 (2006).
10. M. Takizawa, H. Wadati, K. Tanaka, and M. Hashimoto, Phys. Rev. Lett. **97**, 057601 (2006).
11. S. S. Seo, W. S. Choi, and H. N. Lee, Phys. Rev. Lett. **99**, 266801 (2007).
12. A. Rastogi and A. K. Kushwaha, Adv. Mater. **22**, 4448 (2010).
13. H. W. Jang and D. A. Felker, Science **331**, 886 (2011).
14. A. Rastogi and J. J. Pulikkotil, Phys. Rev. B **86**, 075127 (2012).
15. W. Schottky, Phys. Z. **31**, 913 (1930).
16. C. Wang, J. Shao, Z. Mu, W. Liu, and G. Ni, Chin. Opt. Lett. **12**, 040402 (2014).

17. D. Kabra, T. B. Singh, and K. S. Narayan, Appl. Phys. Lett. **85**, 5073 (2004).
18. A. I. Nusir, A. M. Hill, M. O. Manasreh, and J. B. Herzog, Photon. Res. **3**, 1 (2015).
19. Y. Wang, N. Li, P. Duan, J. Deng, L. Zhang, B. Chu, and Q. He, Chin. Opt. Lett. **13**, 060701 (2015).
20. C. Q. Yu, H. Wang, S. Q. Xiao, and Y. X. Xia, Opt. Express **17**, 21712 (2009).
21. H. Águas, L. Pereira, D. Costa, E. Fortunato, and R. Martins, Opt. Mater. **27**, 1088 (2005).
22. A. Ohtomo, D. A. Muller, J. L. Grazui, and H. Y. Hwang, Appl. Phys. Lett. **80**, 3922 (2002).